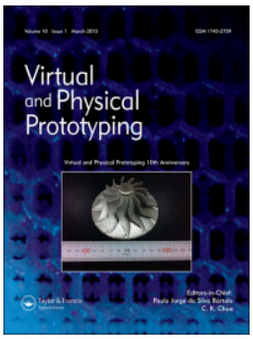

Virtual and Physical Prototyping

ISSN: (Print) (Online) Journal homepage: www.tandfonline.com/journals/nvpp20

Development of a porcine decellularized extracellular matrix (DECM) bioink for 3D bioprinting of meniscus tissue engineering: formulation, characterisation and biological evaluation

Filip Porzucek, Monika Mankowska, Julia Anna Semba, Piotr Cywoniuk, Adam Augustyniak, Anna Maria Mleczko, Ana Margarida Teixeira, Pedro Martins, Adam Aron Mieloch & Jakub Dalibor Rybka

To cite this article: Filip Porzucek, Monika Mankowska, Julia Anna Semba, Piotr Cywoniuk, Adam Augustyniak, Anna Maria Mleczko, Ana Margarida Teixeira, Pedro Martins, Adam Aron Mieloch & Jakub Dalibor Rybka (2024) Development of a porcine decellularized extracellular matrix (DECM) bioink for 3D bioprinting of meniscus tissue engineering: formulation, characterisation and biological evaluation, Virtual and Physical Prototyping, 19:1, e2359620, DOI: 10.1080/17452759.2024.2359620

To link to this article: https://doi.org/10.1080/17452759.2024.2359620

VIRTUAL AND PHYSICAL PROTOTYPING
2024, VOL. 19, NO. 1, e2359620 (14 pages)
https://doi.org/10.1080/17452759.2024.2359620

Taylor & Francis
Taylor & Francis Group

Development of a porcine decellularized extracellular matrix (DECM) bioink for 3D bioprinting of meniscus tissue engineering: formulation, characterisation and biological evaluation

Filip Porzucek[a], Monika Mankowska[a], Julia Anna Semba[a,b], Piotr Cywoniuk[a], Adam Augustyniak[a], Anna Maria Mleczko[a], Ana Margarida Teixeira[c,d], Pedro Martins[d,e], Adam Aron Mieloch[a] and Jakub Dalibor Rybka[a]

[a]Center for Advanced Technology, Adam Mickiewicz University, Poznan, Poland; [b]Faculty of Biology, Adam Mickiewicz University, Poznan, Poland; [c]Faculty of Engineering, University of Porto, Porto, Portugal; [d]Institute of Science and Innovation in Mechanical and Industrial Engineering, LAETA, Porto, Portugal; [e]i3A, Universidad de Zaragoza, Zaragoza, Spain

ABSTRACT

This study aims to present an easily scalable, cost-efficient process of dECM extraction from porcine meniscus, dedicated to bioink preparation and 3D bioprinting. Due to its cartilage like structure and mechanical robustness, the meniscus is an exceptionally demanding tissue for extraction and decellularisation of its ECM. Its processing poses a great difficulty and renders the methods previously developed for soft tissues useless. A process, combining homogenisation, hydrolysis, supercritical CO2 (scCO2) extraction and lyophilisation, was developed to meet this challenge. This protocol allows for retaining its native compounds and biocompatibility while offering good printability and providing a stimulatory environment for cell proliferation and differentiation towards a meniscus-like phenotype. Also, this process is economically and ecologically friendly since it doesn't require the use of high amounts of solvents, detergents or expensive enzymes (DNase). The decellularisation process has been meticulously studied, demonstrating a substantial reduction in DNA content but still exceeding accepted thresholds. The study further explores the biocompatibility of the dECM, demonstrating no detrimental effects of remnant DNA on cell survival during extended in vitro culture, indicating excellent biocompatibility. These findings challenge the current definition of decellularisation effectiveness based solely on DNA content, proposing a broader assessment of biological effects.

ARTICLE HISTORY
Received 6 February 2024
Accepted 8 May 2024

KEYWORDS
Extracellular matrix; decellularization; 3D bioprinting; porcine-derived biomaterials; ASC differentiation

Highlights

- A novel approach for porcine menisci dECM extraction and biocompatible bioink formulation with physicochemical properties suitable for 3D bioprinting is proposed
- The protocol allows for large-scale, detergent-free production of dECM from porcine meniscus, presents the first use of supercritical CO_2 extraction for the preparation of dECM from this elastic and rigid tissue and vastly decreases the processing time
- The results indicate, that mechanotransduction and dECM are insufficient for chondrogenesis induction of adipose-derived mesenchymal stem cells (ASC) - additives enhancing differentiation are required
- Regarding 3D bioprinting of meniscus implants, ASCs cultured in spheroids are not superior to cells cultured in 2D

Introduction

The meniscus plays an indispensable role in articular surface protection, shock absorption, and stress transmission in the knee. Its injuries are incredibly prevalent, reaching 0.7 per 1000 people in the general population, 3.5 in healthy young adults, and even up to 8.27 when considering active-duty military cohorts [1–3]. The studies show a correlation between injury risk and BMI, also highlighting increased rates of athlete-related cases, of which 63.8% required surgical intervention [3,4]. Due to limited vascularisation, the regenerative capability of the meniscus is relatively low and restricted to the outer, vascularised region. The most commonly performed treatment involves suturing or removal via partial or total meniscectomy. However, meniscectomy significantly increases the incidence of osteoarthritis later in life by elevating contact pressure on the tibial

CONTACT Jakub Dalibor Rybka jrybka@amu.edu.pl Center for Advanced Technology, Adam Mickiewicz University, Poznan, Poland
Supplemental data for this article can be accessed online at https://doi.org/10.1080/17452759.2024.2359620

plateau. Approximately 50% of patients with meniscal injuries develop osteoarthritis within 10–20 years after the surgery [5]. Therefore, new treatment options restoring the meniscus's physiological functions are needed [6].

3D bioprinting is a rapidly growing field of regenerative medicine that offers the possibility to regain the physiological functions of an organ without resorting to artificial implants [7]. This technology provides an unparalleled opportunity to design and fabricate meniscal constructs, faithfully mimicking the complexity of its native architecture with patient-specific geometry [8].

There are three main techniques exploited in 3D bioprinting: extrusion, jetting, and vat photopolymerization, differing in the technology of bioink deposition and generation of the desired 3D object. In extrusion-based printing, bioink is extruded from the nozzle, using pressure or a physical piston. A broad range of materials with different mechanical properties and viscosity (10–10^{13} mPas) can be used, as well as high cell densities (up to 10^7 cells/mL). To obtain an optimum resolution (100-200 µm), proper processing conditions (e.g. flow rate and deposition velocity) and bioink properties – a shear thinning behaviour is required [9,10]. Material jetting is a process in which droplets of build material are selectively deposited onto a build bed. Due to the droplet formation process, inks must present a viscosity lower than 15 mPas and cell density should be also lower than 10^6 cells/ml. In the case of acoustic systems, cell viability is limited by the level of frequencies used. Resolution ranges between 20 and 100 µm [11,12]. In vat polymerisation printing (VPP), a container filled with cell-hydrogel suspension is subjected to selective curing (with light or laser) of polymer to form 3D structures. It is characterised by high printing resolution (80–140 µm) and high cell density but has relatively low printing efficiency and a limited range of viscosities [13].

Bioprinting of the meniscus requires optimised conditions that will provide high accuracy, integrity, and durability of printed objects while simultaneously providing an optimal microenvironment for cell growth and proliferation [14,15]. The decellularized extracellular matrix (dECM) obtained from porcine menisci was selected as a candidate biomaterial to fulfil these requirements [16].

Emerging studies demonstrate that ECM-based scaffolds can provide a favourable regenerative microenvironment, promote tissue-specific remodelling, and act as an inductive template for the repair and functional reconstruction of skin, bone, nerve, heart, lung, liver, kidney, small intestine, and other organs [17–20]. Taking into consideration the complex molecular composition of the meniscal ECM, extraction of porcine meniscal ECM is a promising approach, capable of providing printable, natural biomaterial with properties and compositions similar to human native tissue [21]. With appropriate processing, dECM can form a 3D printable hydrogel [22]. The availability of porcine menisci combined with the low risk of immune response stemming from the decellularization process makes it an ideal material for the creation of meniscal scaffolds [23]. Nonetheless, several concerns regarding dECM of animal origin have been raised [14].

Many chemical and physical decellularization processes have been proposed to efficiently isolate the ECM of a tissue from its inhabiting cells while maintaining the biochemical and biomechanical properties of the native tissue. In most of the decellularization protocols detergents such as sodium dodecyl sulfate, sodium deoxycholate, and Triton X-100 are used [24,25]. However, these methods have several drawbacks: (1) time-consumption, (2) ECM proteins denaturation, affecting the mechanical properties, (3) glycosaminoglycans removal (GAGs), which are crucial for creating a proper environment for recellularization, and (4) often fail to remove residual detergent that can provoke cell cytotoxicity [26–29]. Hence, CO_2 in a supercritical state ($scCO_2$) has received attention as a an alternative strategy for tissue decellularization to potentially overcome these problems. The supercritical state refers to a carbon dioxide above its critical temperature and critical pressure, rendering them a very effective solvent because of a unique blend of properties: (1) density similar to liquids, while diffusivity and viscosity similar to gases, (2) minimal surface tension, allowing penetration of pores and surface openings without damaging them, (3) evaporation upon depressurisation, which means there is no residual solvent left (4) chemical inertion, non-toxicity, and non-flammability, which are all significant safety and environmental advantages, (5) low critical conditions (31°C; 7.40 MPa), that do not alter the native structure of proteins, (6) sterilisation properties. Altogether, it makes $scCO_2$, in contrast to detergents, very well-suited for biomaterial extraction and subsequent tissue engineering purposes what has been reflected in the $scCO_2$ use in the extraction of ECM from various tissues [28,30–36]. However, up to date, there has been no publications concerning $scCO_2$ application in ECM isolation from the meniscal tissue.

This work aimed to develop a scalable method of porcine meniscal ECM extraction, retaining its native properties and biocompatibility, while offering good printability, and providing a stimulatory environment for cell proliferation and differentiation toward meniscus-like phenotype. Since the meniscus is cartilage-like, highly elastic, and rigid tissue, its processing poses a great challenge and renders the methods previously

developed for soft tissues useless. To meet this challenge, a process combining homogenisation, hydrolysis, supercritical CO_2 ($scCO_2$) extraction, and lyophilisation was developed. This combination of steps allowed for obtaining dECM-based bioink, which retained most of its native compounds while gaining very good 3D bioprinting properties. To evaluate the chondrogenic potential of the dECM-based bioink, scaffolds were bioprinted either with suspended adipose-derived mesenchymal stem cells (ASC) or 3D spheroids composed of the same cell line, which have been demonstrated to mimic tissue microenvironment more closely than monolayer cultures by recapitulating 3D architecture and enabling spatial cell-cell and cell-ECM interactions [37,38].

Materials and methods

dECM preparation from porcine menisci

Porcine menisci were collected at a local slaughterhouse, frozen, and stored at – 20°C for further processing. The dECM was prepared according to patent application no. P.441935. One kilogram of porcine menisci was separated from tendons and fat residues, followed by washing with deionised water. Tissue was minced in an electric meat mincer using a cutting plate with a hole size of 8 mm, and again using a 6 mm hole size. Minced tissue was subjected to the water extraction process at room temperature (RT) overnight, under continuous mechanical stirring. The solid phase was separated and the second extraction was performed in 0.05M lactic acid at RT overnight under continuous mechanical stirring. Following filtration bag separation, the solid phase was subjected to hydrolysis in pepsin (Sigma-Aldrich) solution. After 48 h of hydrolysis, conducted at RT under continuous mechanical stirring, solid residues were filtered out with the filtration bag. The hydrolysis step was repeated three times. In the next step, the filtrate was subjected to a lyophilisation process (74 h under the pressure of 1 mBar, 8 h under 0.18 mBar). To obtain fine, easily dissolvable powder for bioink formulation, the lyophilised material was cryo-milled with the 6875 Freezer/Mill High Capacity Cryogenic Grinder (SPEX). The samples were pre-cooled in grinding vials by immersing in liquid nitrogen for 5 min and subjected to three cycles of cryo-milling (grinding time: 5 min grinding at 15 cps with a 2 min intercool for each cycle) and then sieved through a 300 µm strainer. Subsequently, two variants – with or without a DNase treatment, followed by supercritical CO_2 extraction were tested ($DscCO_2$ vs. $scCO_2$). In the $DscCO_2$ variant, pH was adjusted to 7.5, and incubated with 25 U/ml of DNase (A&A Biotechnology) in PBS at 37°C for 24 h. In the next step, three cycles of centrifugation and washing in deionised water were performed. In both variants, supercritical CO_2 extraction was applied with the use of Spe-ed™ SFE-2 Supercritical System (Applied Separations). The dECM was loaded into the extraction vessel (50cm^3). CO_2 was compressed to 300 bar and heated to 40°C to reach the supercritical state. Then, anhydrous ethanol was supplied to reach a concentration of 20%. Batch extraction was performed for 20 h, followed by one-hour continuous extraction at flow rates of 5 l/min and 0.5 ml/min for CO_2 and anhydrous ethanol respectively. After the extraction, the decompression step at a flow rate of 20 l/min was performed. The extraction vessel was unsealed under a laminar flow hood to prevent contamination.

Biochemical analysis

DNA was isolated with Genomic Micro AX Tissue Gravity DNA kit (A&A Biotechnology) according to the manufacturer's protocol and measured with Qubit 4.0 with the dsDNA BR kit (Thermo Fisher). The agarose gel electrophoresis was performed for qualitative analysis of the isolated DNA. GAG content was calculated based on a colorimetric test – Glycosaminoglycan Assay Blyscan (Biocolour) performed with a microplate reader (Infinite 200 Pro, Tecan) according to the manufacturer's protocol. Collagen concentration was quantified based on hydroxyproline content, assuming it comprises 13.5% of all amino acids [39]. Absorbance at 550 nm wavelength was measured using a Tecan 96-well plate reader. Fat content was measured with the Soxhlet method. For nuclei staining in lyophilised dECM 20 µg/ml Hoechst 33342 solution (Thermo Scientific) was used and samples were analyzed using a confocal microscope (IX83, Olympus).

Bioink formulation and 3D bioprinting

The bioinks were prepared by solubilisation of the UV-sterilized powders (0.75% alginate and 3-7% dECM for dECM-based bioink and 0.75% alginate, 4% gelatine and 1.4% CCNC, that was used as a control, described in our previous work of Semba et al.[40]), in Mesenchymal Stem Cell Growth Medium 2 (PromoCell) supplemented with Supplement Mix, 100 U/ml penicillin, 100 µg/ml streptomycin, and 25 ng/ml amphotericin B. Gelation of the dECM bioink was achieved by adjusting pH with NaOH to a value of 7.5. Human adipose tissue-derived mesenchymal stem cells (ASC) (PromoCell) up to passage 7 were utilised for 3D bioprinting. For spheroid formation, pelleted cells (approx. 500 cells per spheroid) were cultured on an ultra-low attachment culture plate with micropores (Elplasia® 6-well,

Corning). The 3D model was designed in Tinkercad software as a cylinder (6 mm × 2 mm), loaded into the BioX bioprinter (Cellink), and sliced by bioprinter software with the infill set to a 35% rectilinear pattern. Bioinks were gently mixed with ASC cell suspension to a final concentration of 7.5×10^6 cells/ml or 11,500 spheroids/ml. Based on resolution and shape fidelity analysis, the bioprinting parameters were selected and adjusted to a 22G nozzle (inner diameter 410 µm). 3D bioprinted constructs were crosslinked with sterile 200 mM CaCl2 in 4.6% D-mannitol, for 10 min at RT and cultured in vitro 37°C, at 5% CO2 atmosphere. Depending on the experiment DMEM low glucose with 10%FBS, Mesenchymal Stem Cell Growth Medium 2 (PromoCell), Mesenchymal Stem Cell Chondrogenic Differentiation Medium (Promocell) and our home-made medium formulation comprised of DMEM low glucose with 10% FBS, 50 µg/ml 2-phospho-L-ascorbic acid, 100 ng/ml dexamethasone, 10 ng/ml TGF-β1, and antibiotics (100 U/ml penicillin, 100 µg/ml streptomycin, and 25 ng/ml amphotericin B) were used.

Rheology

The rheological characterisation was performed on the MCR 302 instrument (Anton Paar) equipped with 25 mm, smooth, parallel plates (PP25) and a 1 mm gap setup. The following tests were carried out: amplitude sweep test, temperature sweep test, and rotation. The oscillatory measurement was divided into successive intervals: a pre-shear step (constant strain amplitude (γ) of 0.01% and angular frequency (ω) of 10 1/s), a rest time (10 min), and an amplitude sweep test (strain amplitude 0.01% – 500% and constant angular frequency 1 rad/s). Temperature sweep measurements were made at a rate of 2°C/min in temperature ranging from 20°C to 40°C. In the rotation study, the shear rate range was set from 0.01 1/s to 1000 1/s. A layer of silicone oil was applied on the sample surface to prevent water evaporation.

Scanning electron microscope (SEM)

The cylindrical constructs (dimensions 10 mm × 2 mm), were characterised by scanning electron microscope (Quanta FEG 250, FEI) in low vacuum conditions at the pressure of 70 Pa with an electron beam energy of 10 keV. Before analysis, the scaffolds were frozen at – 80° C for 2 h and then lyophilised (Alpha 1–2 LDplus lyophilizer, Christ).

Cell viability

Cell viability and morphology within the constructs were assessed with the LIVE/DEAD assay, and performed according to the producer guidelines (LIVE/DEAD® Viability/Cytotoxicity Kit, Invitrogen). Subsequently, constructs were scanned with a confocal microscope (IX83, Olympus). Middle slices were selected from each of the scans and analyzed with the ImageJ software.

Mechanical characterisation

10-week-old constructs with or without cells were measured before testing for diameter and height and tested using a custom-made machine [41]. All tests were performed at RT, using a two-step protocol – first, a preconditioning step accommodated the sample to the load (10 cycles, 10% strain at 2 mm/min), then the ramp test (60% strain at 2 mm/min). Before each test, the indenter was manually lowered to reach the sample's surface.

The force-displacement experimental data was acquired at a maximum sampling of 100 Hz. Due to fluctuations in the sampling, data from individual samples were regularised by interpolation procedure, to enable proper statistical treatment. The statistics carried out:

1. considers each experimental curve $i \in \{1, \ldots, n\}: i, n \in N$ of the form $c_j^{(i)} = (f_j, d_j)$ with a total of $j \in \{1, \ldots, m\}: j, m \in N$ experimental data points, as an individual experiment
2. considers that all the curves $c^{(i)}$ describe the same phenomenon – the same testing protocol is applied to *(n)* identical samples corresponding to the experimental batch.

After the data regularisation (via interpolation), it is possible to apply a point-wise statistical treatment to the curves of a given batch, allowing us to calculate a mean curve $c^{(mean)}$ representative of the whole batch, made of the point-wise means, carried over the n curves for each point *j* and statistical quantities such as the standard deviation (SD) and the standard error of the mean (SEM). The mean results *(f, d)* can be converted to stress-strain (σ, ε) given that all samples are from the same material and have the same geometry. Assuming the stress-strain mean curve, stiffness estimation was carried out considering the slope of the first linear region.

Gene expression analysis

Constructs were homogenised in 800 µl of Fenozol with zirconia/silica beads (Bead-Beat Total RNA Mini kit, A&A Biotechnology) in a tissue homogeniser (Precellys 24, Bertin) for 30 s. Samples were heated to 50°C for 5 min, supplemented with 200 µl of chloroform, and centrifuged. The aqueous phase mixed 1:1 with isopropanol

was transferred on microcolumns and RNA was purified according to the producer's protocol (Clean-Up RNA Concentrator, A&A Biotechnology). After isolation, RNA was reverse-transcribed into cDNA (High-Capacity cDNA Reverse Transcription Kit, Applied Biosystems). For gene expression analysis Maxima SYBR Green/ROX qPCR Master Mix, Applied Biosystems, and QuantStudio™ 7 Flex (Applied Biosystems) were used. Relative expression was calculated with ddCt, referred to as RPS29 gene expression, and normalised to the average expression of the gene for a particular construct variant on day 1. The list of dedicated primer pairs is presented in Supp. Table 1.

ELISA analysis

Media from bioprinted constructs were collected after 8 weeks of culture and frozen at – 20°C for further experiments. ELISA Kit (FineTest) for human collagen type I, type II, type VI, and type X, along with aggrecan (ACAN), cartilage oligomeric matrix protein (COMP), and matrix metallopeptidase 13 (MMP13) were performed according to the manufacturer's protocol. Absorbance was measured at 405 nm using a microplate reader (TECAN). All experiments were performed in six biological and two technical repetitions.

Immunofluorescence analysis

Slices of bioprinted constructs were cryopreserved in OCT (VWR) and cut to 30 µm at – 20°C. Samples were fixed with 4% paraformaldehyde (Merck) followed by permeabilization with 0.5% Triton X-100 (Merck) solution and blocking with 10% goat serum (Merck) in 0.1% Triton X-100. The slices were incubated overnight at 4°C with three primary antibodies simultaneously – anti-collagen I antibody conjugated with biotin (Invitrogen 600-406-103), anti-collagen II antibody (Abcam ab185430), and anti-aggrecan antibody (Invitrogen PA5-32650). The next day samples were washed and incubated with: 0.2 µg/ml streptavidin-FITC conjugate (ThermoFischer), 1:1000 anti-mouse IgG conjugated with Cy5.5 fluorophore (Abcam); and 1:1000 anti-rabbit IgG conjugated with TexasRed fluorophore (Abcam). Subsequently, slices were washed and immersed in a DAPI solution with fluoroshield (Merck) and sealed. Immunofluorescence was visualised under a confocal microscope (IX83, Olympus).

Statistical analysis

For statistical analysis and graph preparation, the GraphPad Prism 8.0.1 software was used. One-way ANOVA was applied for statistical calculation of viability from at least 5 replicates, while two-way ANOVA for analysis of printing accuracy from 4 constructs in each group. Statistics for gene expression analysis were calculated with t-Student's test from at least 2 (up to 6) replicates.

Results

Preparation and characterisation of ECM obtained from porcine menisci

The three critical steps of our original protocol for ECM extraction were extraction of water – and acid-soluble ECM components, protein digestion, and final decellularization – which combined DNase treatment and extraction in scCO2 (Figure 1A). Collagen, GAGs, and DNA content were measured at each stage of the procedure (Supp. Table 2). First, the extraction at neutral pH was performed, preserving the GAGs and collagen while removing 16.2% of the DNA content. The second extraction conducted in acidic pH resulted in a further decrease in DNA content (to 58.6% of initial value) and noticeable GAGs depletion (to 70.6%) while the collagen content remained constant (Figure 1B). Along with considerable changes in DNA content, severe DNA fragmentation was observed (Supp. Figure 1). In comparison to the native tissue, the dECM after pepsin digestion comprised 79.7% collagen (584.3 ± 25 µg/mg), 51.7% GAGs (15.1 ± 1.4 µg/mg), and 45.3% DNA (222 ± 8.7 ng/mg). Since the amount of DNA in the dECM exceeded the recommended minimum standards for biomedical material, additional decellularization steps were added [42]. Two variants: with or without DNase treatment, followed by supercritical CO2 extraction were tested (DscCO2 or scCO2, respectively) (Figure 1A). While collagen and GAG content were maintained at high levels (96.1% and 69.7%, respectively), the DNase treatment caused a considerable decrease in the DNA content (22.7 ± 1.5 ng/mg, 4.6%) (Figure 1B). The scCO2-only variant resulted in similar outcomes in terms of collagen and GAG concentration (92.2% and 59.9%, respectively), but the DNA content decreased only to 37.7% (184.7 ± 6.8 ng/mg) of its starting value. Hoechst 33342 staining revealed numerous, rounded nuclei in the native, pulverised meniscus tissue, while in the extracted dECM (regardless of DNase use) nuclei showed deterioration and a significant decrease in number (Supp. Figure 2). Agarose gel electrophoresis indicated severe fragmentation of the DNA isolated from the dECM, even before DNase or scCO2 treatment (Supp. Figure 1). scCO2 extraction allowed for a substantial decrease of lipid content (to 0.5% ± 0.2%) in the dECM compared to native tissue as well as to extracted and hydrolyzed

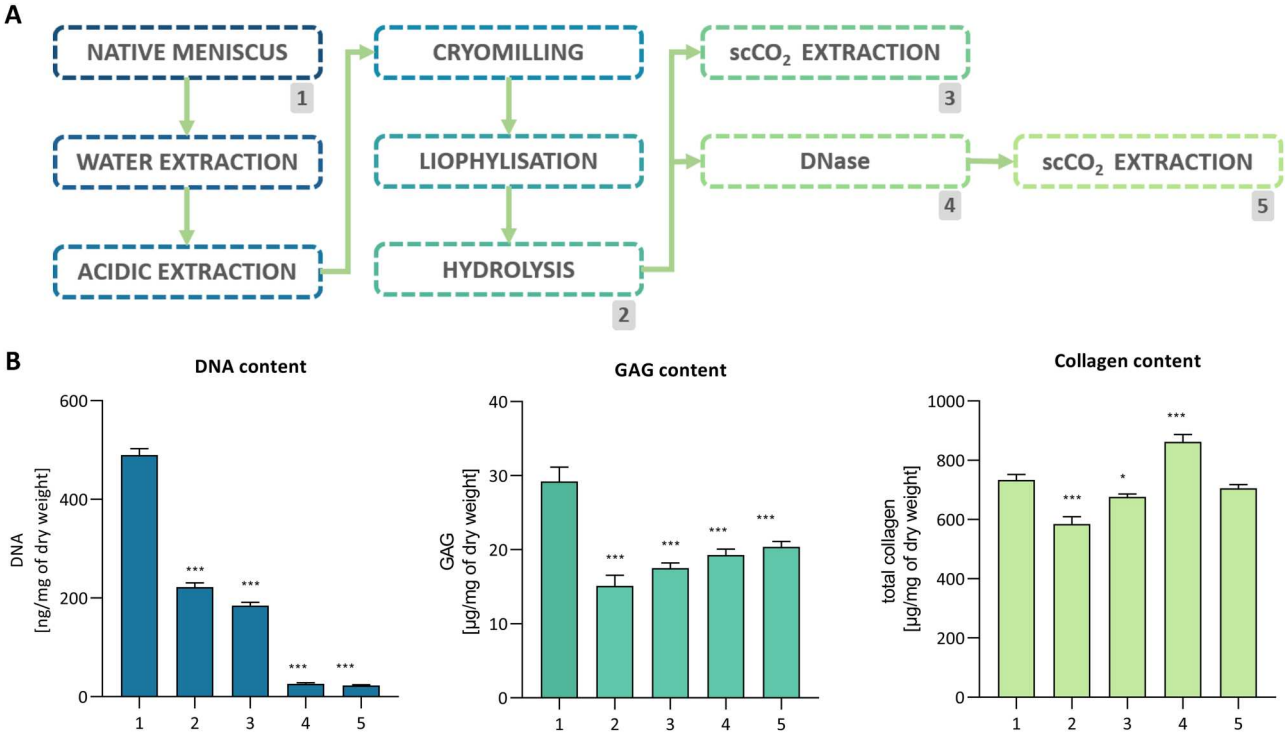

Figure 1. Manufacturing and decellularization of the dECM obtained from the porcine meniscus. **1 –** native meniscus; **2** – hydrolyzed dECM; **3** – $scCO_2$ variant; **4** – hydrolyzed, treated with DNase dECM; **5** – $scCO_2$ variant. **A.** Process flow diagram. **B.** DNA, GAG, and collagen content (n = 3; P* < 0.05, P*** < 0.001).

dECM (6.66% ± 0.26 and 1.69% ± 0.17% respectively). Due to the costs of the DNasing process and significant material losses, only dECM treated with scCO2 – not with DNase – was used in the following experiments.

dECM-bioink characterisation

Since the 1% and 3% dECM bioinks were too liquid and 5% dECM exhibited poor printability (data not shown), a concentration of 7% was selected for further studies. The gelation in RT was induced by adjusting the pH of the bioink from 2.5 (optimal for pepsin activity) to the value of 7.5. Rheological analysis revealed that the amplitude sweep curve of the 7%dECM bioink has a shorter linear viscoelastic region (LVE) in comparison to gelatine-based bioink (Figure 2). It means that 7% dECM bioink is more sensitive to microstructure changes under increasing strain. The inclusion of gelatin or the CCNC, which increases the stiffness of gelatine-based bioink, may be the cause of this divergence. Nevertheless, both examined bioinks displayed G′ > G″ in the LVE area, indicating that the samples are viscoelastic materials with a gel-like or solid structure. The observed shear-thinning behaviour is desired for bioinks, providing good printability and stability of a printed construct (Figure 2). The 3D printed constructs displayed structural variations as demonstrated via SEM (Supp. Figure 3). In the 7%dECM variant porosity and minuscule channels were noticed, while the gelatine-based variant had no channels.

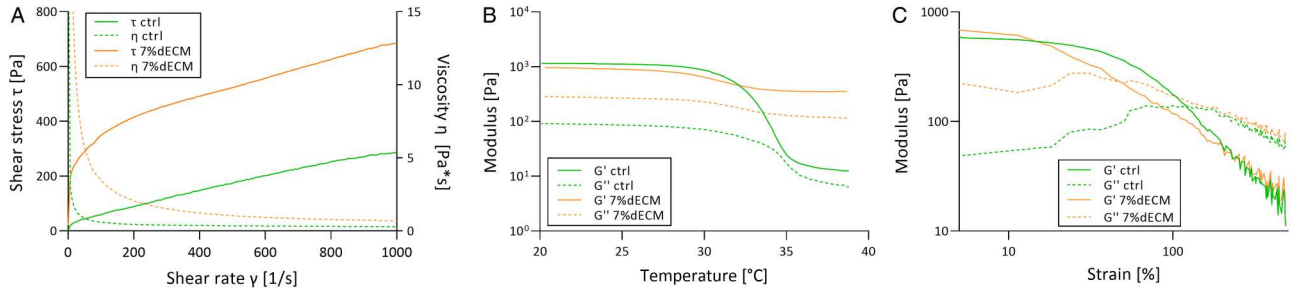

Figure 2. Rheology of the bioinks. **A.** Amplitude sweeps. **B.** Temperature sweeps. **C.** Flow curves.

dECM biocompatibility

Bioinks were used for 3D bioprinting with ASC pre-cultured as monolayers or spheroids. The parameters for bioprinting were set adequately for each bioink (Supp. Table 3). The biocompatibility of the obtained bioinks was assessed based on cell viability analyzed via LIVE/DEAD assay, at four-time points (Figure 3). Analysis was conducted 24 h post printing confirmed that the 3D bioprinting procedure did not affect cell survival nor destroyed the spheroids (Figure 3). Additionally, only a few dead cells were observed over the course of the 30 days of in vitro culture in both tested bioinks, indicating excellent biocompatibility.

Important morphological changes, dependent on the composition of the bioink were observed at different time points (Figure 3). The gelatine-based bioink maintained the oval shape of suspended cells for up to 20 days, after which cell elongation was observed. In the dECM-based bioink, a profound cell elongation was observed as soon as day 10. Spheroids in the gelatine-based bioink maintained their shape, although a loss of density over time was visible, while in the dECM group, spheroids started to decompose at day 10. Since red signals were not observed, the decreased number of cells seen on day 30 (Figure 3) is most likely related to cell migration outside of the construct rather than to cell deaths.

Evaluation of chondrogenic properties of dECM-based bioink

Due to the previously reported stimulatory properties of an ECM microenvironment toward stem cell differentiation, the chondroinductive potential of the obtained dECM-based bioink was investigated [43,44]. With regard to gene expression levels an interesting expression pattern was observed in both analysed bioink variants and both types of cell pre-cultures: significant elevation of transcription level at day 10, followed by an intense decrease in subsequent time

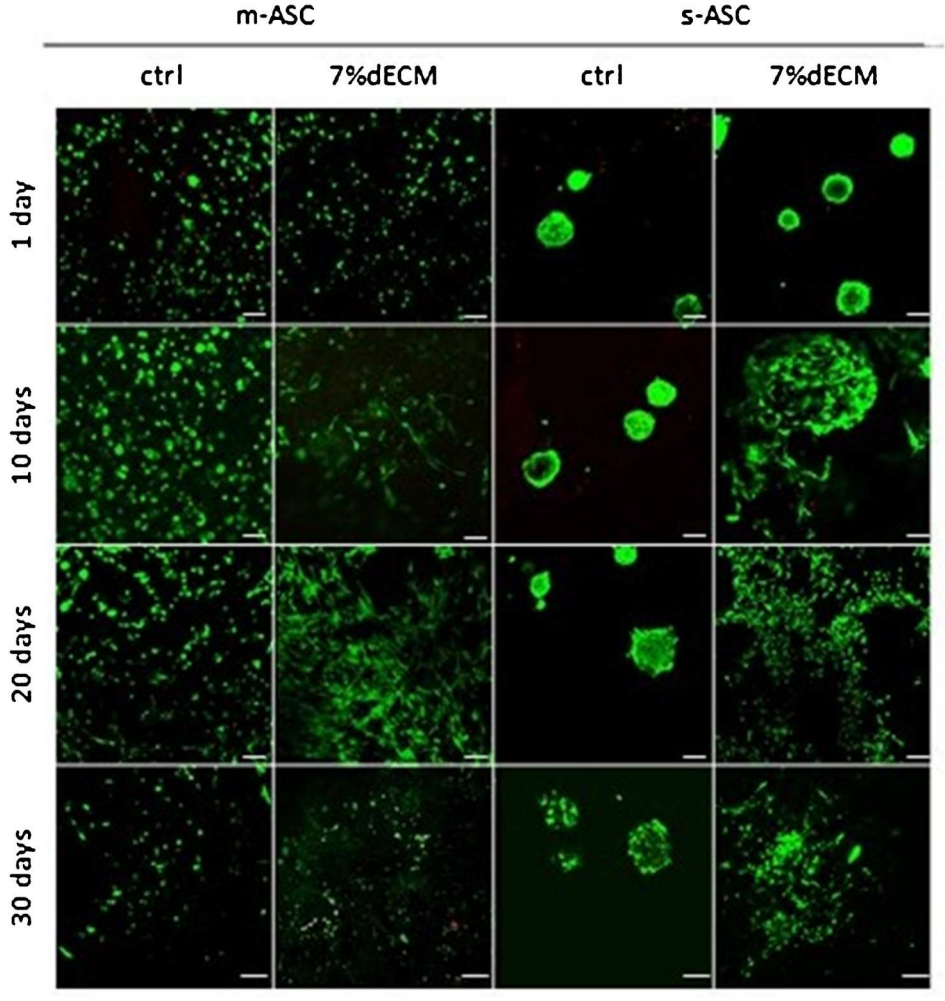

Figure 3. ASC viability determined with the LIVE/DEAD assay. Representative images of m-ASC (pre-cultured as monolayer) and s-ASC precultured as spheroids in the ctrl, and the 7%dECM bioinks (scale bar = 100 µm).

points. This pattern concerned genes encoding collagens (*COL1A1, COL6A1, COL10A1*) and COMP (Supp. Figure 4). Similar behaviour has also been observed for chondrogenic markers CDH2 and SOX9 in 7%dECM (Supp. Figure 4) while in gelatine-based bioink the increase occurred later, at day 30. In both bioinks, SOX5 increased significantly at day 30. Such a recurrent pattern might suggest time-dependent accumulation of changes in mesenchymal stem cells which are undergoing reprogramming toward chondrocytes, yet require stronger induction. Unexpected changes in gene expression at day 10 are parallel with the observed cell elongation.

Although other studies point toward the advantageous properties of cells pre-cultured as spheroids over those pre-cultured in monolayer for tissue engineering, in our experiments both cultures maintained high viability (Figure 3), while RT-qPCR analysis did not prove the superiority of spheroid cell pre-culture regardless of bioink variant [45] (Supp. Figure 4).

To evaluate the dECM impact on ASC synthesis of ECM components the immunofluorescence assays for three key proteins of cartilage – collagen type I, collagen type II, and ACAN – were performed. After 8 weeks of in vitro culture, in both types of bioink, significant enhancements in signal intensity originating from all three examined proteins were observed (Figure 4). The higher production of ECM proteins was noted in constructs based on the dECM. Again, spheroid culture superiority was not proven (Figure 4).

Subsequently, we assessed the concentration of proteins secreted by cells into the medium, focusing on the key cartilage ECM proteins: ACAN, COMP, collagen type I, II, VI, X, and MMP 13 (Figure 5). The profound increase, with time, was observed for ACAN, consistently across all tested variants (gelatine-based and 7%dECM as well as pre-culture types), reaching the highest values for 7%dECM – based bioink. The tendency for increasing production was also noted for COL I and COL VI, with slightly higher levels in gelatine-based bioink. Collagen type X displayed relatively steady expression levels in all analyzed variants. The MMP13 and collagen type II were undetected, while COMP either remained undetected or revealed low concentrations (< 6 ng/ml).

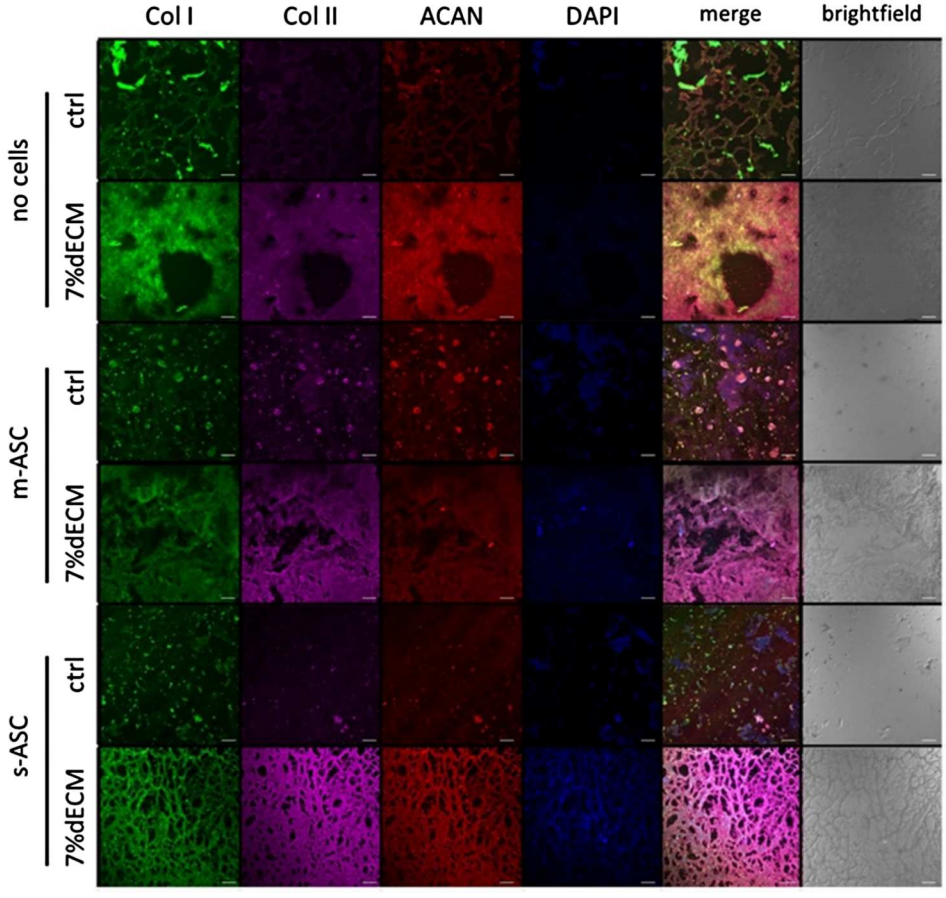

Figure 4. Production of ECM components by ASCs within bioprinted constructs. Representative images of constructs bioprinted with bioinks based on 7%dECM and gelatine-based (ctrl) after 8 weeks of culture. m-ASC – constructs with cell precultured as monolayer, s-ASC – constructs with cells precultured as spheroids.

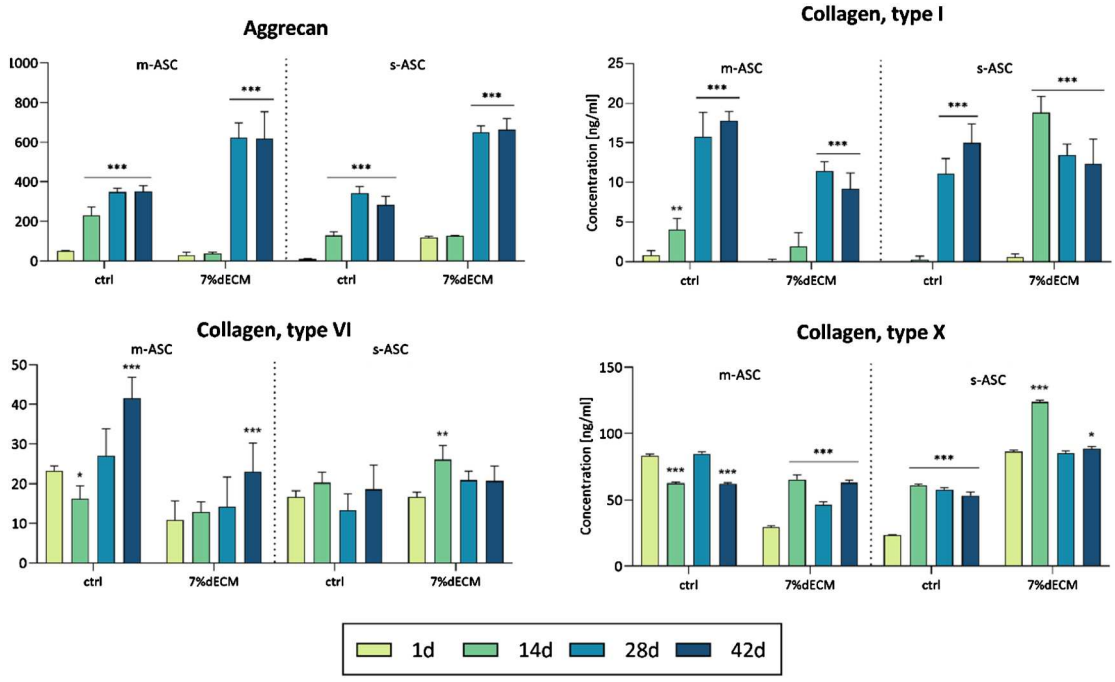

Figure 5. ELISA analysis of proteins secreted by cells into the medium. The cells (m-ASC or s-ASC) were embedded in construct bioprinted with ctrl or 7%dECM at 24 h, 14, 28, and 42 days post-printing. The statistical significance was determined by 2-way ANOVA and calculated for a particular time point compared to day 1 ($n \geq 3$; $P^* < 0.05$; $P^{**} < 0.01$ and $P^{***} < 0.001$).

Only in the case of COL I and X, the spheroid cultures performed better.

Within the studied strain range (0-5%), based on Young's modulus derived from the initial linear segment of the stress/strain curves, constructs bioprinted with gelatine-based bioink were found to be softer than the bioprinted with 7%dECM ones (Figure 6). Although both variants become stiffer when cultured with cells, the gelatine-based surpassed the 7%dECM in stiffness. Notably, Young`s modulus of gelatin-based constructs increased by more than double when compared to constructs without cells.

Subsequently, we aimed to assess whether 3D bioprinted ASC, under the influence of various chondroinductive media, would exhibit increased production of collagen type I, type II, and ACAN. For that purpose, 7%dECM constructs were cultured in three media: DMEM low glucose with 10%FBS, Mesenchymal Stem Cell Chondrogenic Differentiation Medium (Promocell), and our custom-made medium formulation including DMEM low glucose with 10% FBS, 50 µg/ml 2-phospho-L-ascorbic acid, 100 ng/ml dexamethasone, 10 ng/ml TGF-β1, and antibiotics (100 U/ml penicillin, 100 µg/ml streptomycin, and 25 ng/ml amphotericin B). A noticeable rise in the signal intensity for all three studied proteins was observed (Figure 7), with the

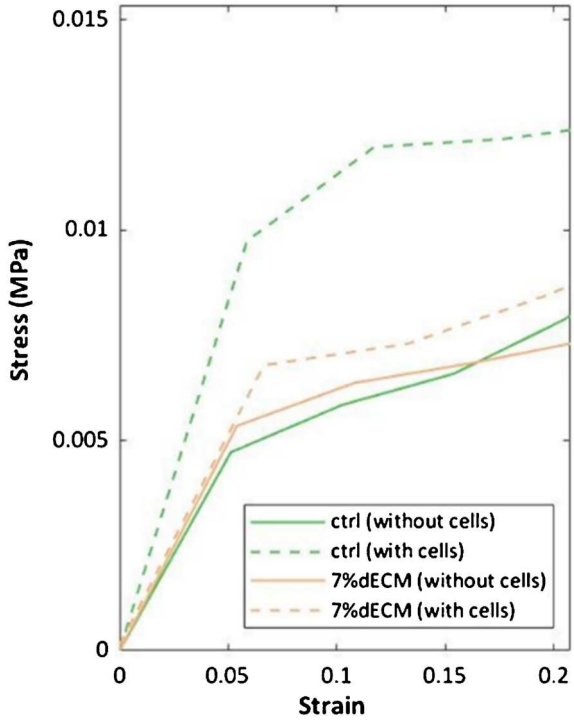

Figure 6. The stress-strain curves of constructs bioprinted with different bioinks (ctrl, 7%dECM) both with and without cells. The measurements were taken within 24 h after production for cell-free constructs, while constructs with m-ASC were assessed at 10 weeks of culture.

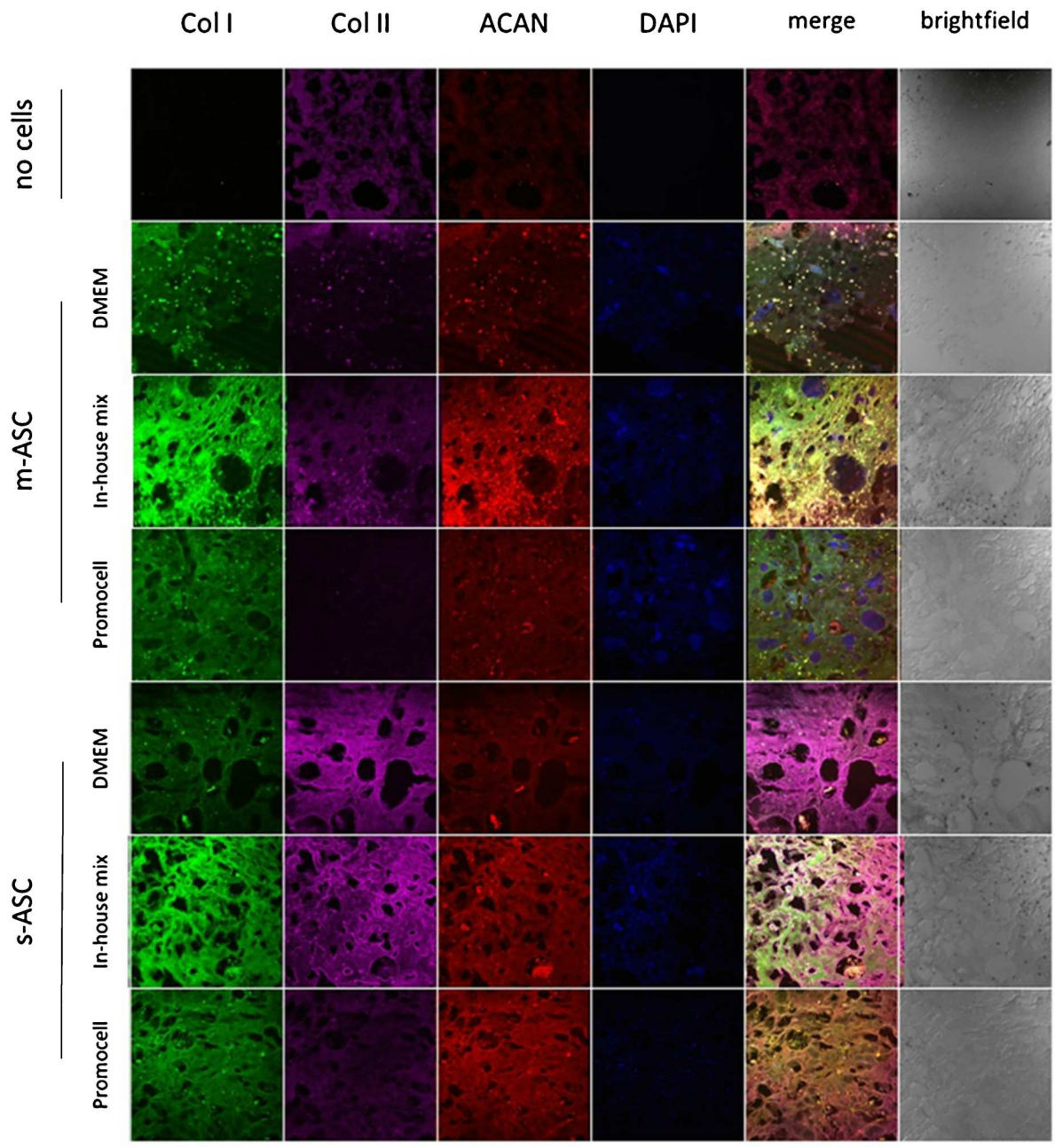

Figure 7. Production of ECM components by ASCs within bioprinted constructs. Representative images of bioinks based on 7%dECM cultured in media **DMEM** – control media DMEM low glucose with 10% FBS; **in-house mix** DMEM low glucose with 10% FBS, 50 µg/ml 2-phospho-L-ascorbic acid, 100 ng/ml dexamethason based one, 10 ng/ml TGF-β1, and antibiotics (100 U/ml penicillin, 100 µg/ml streptomycin, and 25 ng/ml amphotericin B); **Promocell** – Mesenchymal Stem Cell Chondrogenic Differentiation Medium (Promocell).

most pronounced increase in the custom-made medium.

Discussion

Meniscus, which represents the hard and elastic tissue type, presents significant processing challenges, making most of the existing procedures ineffective. In this study, an innovative, detergent-free approach to bioink formulation from decellularized porcine meniscus ECM has been proposed. It allows for a large-scale and cost-efficient ECM extraction from easily accessible slaughter stock. A single batch enables the processing of 2 kg of raw meniscus in laboratory conditions (20-liter vessel) in a 10-day course (including lyophilisation time), resulting in 250 g of dECM powder. In contrast to many published protocols, which require manual tissue slicing/cutting, in this protocol the industrial meat grinder has been applied, substantially reducing the time required for dECM preparation. The

introduction of extraction under native conditions increases the microbiological purity of the material and enables the acquisition of native proteins before their enzymatic hydrolysis. Noteworthy, moving cryogenic milling and supercritical extraction to the final stages has increased process efficiency. For instance, to obtain 250 g of dECM, when the raw meniscus is decellularized via supercritical extraction, 4 rounds of supercritical extraction (using a 1-liter vessel) would be required. When supercritical extraction is introduced at the final stages, decellularization of pre-treated tissue can be performed in 2 rounds. Taken together, introduced modifications improve the ecological (no detergent usage) and economical (reduced proteolytic enzyme amounts required) aspects of the process as well as reduce the time of the workflow.

The protocol proposed in this work retained a substantial amount of ECM components – 92.2% of collagen and 59.9% of GAGs. In comparison, in other studies on ECM extraction from porcine meniscus, the retention of collagen was comparable with our results (88.7%), while GAGs content was significantly reduced to 30.9%. Our method provided the highest retention of ECM components present in native tissue [46]. In other studies on tendon and cartilage decellularization authors also reported a substantial loss of GAGs (retention of 30% and 13%, respectively)[47]. Since it has been established that GAGs play an important role in maintaining the compressive stiffness and load-bearing capabilities of articular cartilage, the need for maximal GAGs retention in the decellularization process is evident [48].

DNA content in the DNase-treated variant was reduced by 96.4% (to 22.7 ± 4.6 ng/mg) compared to native tissue, while the $scCO_2$ alone variant resulted in a reduction of 62.3% (to 187 ± 6.8 ng/mg). It has to be emphasised that most of the reduction was achieved during water/acidic extraction and pepsin digestion steps – from 489 ± 12.9 ng/mg to 222 ± 8.7 ng/mg, while the subsequent step of $scCO_2$ extraction diminished the DNA content further by only ~37 ng/mg. Despite successful use in other issues (e.g. skin and nerves [49,50], those results are in accordance with work on cartilage by Antons et al., where low effectiveness of $scCO_2$ extraction for DNA removal was demonstrated [47]. Additionally, DNA was heavily degraded in all preparations that involved extraction stages before pepsin digestion, indicating the importance of this step for decellularization. Histologically, in all studied extraction variants cell nuclei were mostly removed, while the morphology of the remaining nuclei indicated their degradation. Also, the number of visible nuclei decreased in comparison to pulverised native tissue. Similar results were presented by Antons et al. where trace amounts of disrupted nuclei were detected by DAPI staining after the decellularization of cartilage tissue [47]. Eventually, $scCO_2$ extraction did not provide a significant decrease in DNA content in dECM samples. Equally unsatisfying results were reported in other studies concerning the decellularization of elastic tissues – cartilage and tendon – with $scCO_2$ in various homogenisation regimes [51]. In both articles, authors disclose the ineffectiveness of $scCO_2$ when used without pre-treatment, regardless of extraction times or added co-solvents. Importantly, lipid content reduction after $scCO_2$ treatment may be crucial from a clinical standpoint, as lipids were shown to elicit an immune response [52]. For example, studies on face transplant revealed upregulation of genes responsible for lipid presentation (CD1B, CD1C, CD1E) in patients undergoing 3-grade rejection episodes, suggesting that CD1-presented glycolipid antigens may drive processes involved in allorecognition [53].

Currently, the effectiveness of the decellularization process is loosely defined by the DNA content analysis which is a simplistic approach, leaving the question of the biological effects elicited by remnant non-nucleic residues unanswered. The current guidelines are based on studies and observations of adverse host responses to a biomaterial [42]. In the literature, the threshold criteria include: < 50 ng dsDNA per mg of ECM dry weight; < 200 bp DNA fragment length; and lack of visible nuclei in the material stained with DAPI or H&E [42]. In our previous study, the remnant DNA content in a clinically-approved collagen membrane did not elicit an adverse immune response, despite breaching all of the mentioned criteria [48]. These observations were supported by 2-, 5 – and 10-year clinical follow-ups of patients with meniscus injury treated with the membrane via arthroscopic matrix-based meniscus repair (AMMR) [54,55]. Additionally, in the study by Ritchie et. al., mice injected with DNA isolates from porcine ECM (native or processed) demonstrated only a slight elevation of proinflammatory cytokines` levels, while neither full-length dsDNA nor fragments below 500 bp in length caused mice to produce anti-DNA antibodies (even at concentrations many folds greater than expected in a clinical exposure) [56]. Our research proves that the extracted dECM is not only suitable for formulating bioink for 3D bioprinting but also has no adverse effect on cell survival in a long-term *in vitro* culture. The observed change in morphology of ASC bioprinted in 7% dECM – cell elongation from day 10, suggests cell differentiation into fibrochondrocyte-like cells, specific for the red-red meniscal zone. This behaviour is in accordance with other studies demonstrating that a

similar morphology change is stimulated by components derived from the red-red meniscus zone or ECM extracted from porcine meniscus [57,58]. Gene expression analysis supports this thesis, since the presence of mRNA coding chondrogenic markers (*SOX5* and *SOX9*), as well as typical for meniscus tissue ECM components: aggrecan, and collagens, was noted. We have also confirmed the overproduction of collagens and aggrecan in cells 3D bioprinted with 7%dECM bioink with immunofluorescence and ELISA assays. All those results suggest that ASC cultured in constructs with dECM are differentiating into fibrochondrocyte-like cells, typical for meniscus tissue. Mechanical analysis revealed an increase in Young`s modulus of the prints during culture, indicating an ongoing remodelling of the cellular microenvironment. Secretion and sequestration of ECM components is one possible explanation, however, active remodelling may also take place. However, bioink reinforcement, for example with carbon nanotubes, is advised [59].

The peaks in the expression of genes involved in chondrogenesis and chondrocyte metabolism around day 10 of culture, followed by downregulation of mRNA production, suggest a possible transition into a state of quiescence. Additionally, neither dECM nor 3D bioprinting process, via mechanotransduction, seemed to provide effective stimulation for ASC differentiation into chondrocytes. Following this notion we have tested the effect of three differentiation media on collagen and aggrecan production, as a proxy for effective differentiation. In constructs composed of 7%dECM and ASC cultured in the medium formulated from DMEM low glucose with 10% FBS, 2-phospho-L-ascorbic acid, dexamethasone, and TGF-β1 cells exhibited significantly elevated levels of collagen I, collagen II, and aggrecan, surpassing even those observed in the commercial chondrogenic medium. We hypothesise that the *in vitro* culturing of 3D bioprinted constructs containing ASC is necessary prior to transplantation into the recipient and that the ascorbic acid, dexamethasone, and TGF-β1 are efficient chondroinducers.

To conclude, we present an efficient, easily scalable process of dECM preparation from porcine meniscus, which stands out from those previously described in the literature by selecting appropriate methods and the order of their implementation. It is the first detergent-free protocol that instead uses $scCO_2$ for meniscus tissue. Such an approach has allowed us to circumvent of commonly used less effective and time-consuming decellularization strategies, such as detergent treatment and associated washing steps, which are proven to leave remnants of detergents that interfere with cellular activity. Altogether, the proposed approach yields dECM with very high preservation of both collagens and GAGs, sterile, and free from other chemicals. Also, this process is economically and ecologically friendly because it doesn't require the usage of high amounts of solvents, detergents, or enzymes. Nowadays, concern for the environment and the demand for sustainable resources are increasing, and the development of technologies enabling large-scale production is highly valued.

Available data indicates that the immunological safety of porcine ECM-based biomaterials seems to be unrelated to residual DNA content themselves, invalidating the need for extensive processing, which may compromise the material`s bioactive properties. In light of those findings, we proposed the utilisation of the dECM containing residual DNA fragments for 3D bioprinting. The obtained dECM-based bioink was proven biocompatible, maintaining high cell viability, and increased expression and translation levels of proteins involved in chondrogenesis and the deposition of ECM components specific to the meniscus. Our research also indicates the need for additional stimulation of ASC cells differentiation, hence we propose pre-implantation *in-vitro* culturing of 3D bioprinted constructs in a medium containing 10% FBS, ascorbic acid, dexamethasone, and TGF-β1 for enhanced ASC differentiation and production of ECM.

Acknowledgments

Authors would like to thank Katarzyna Hubert, for technical help.

Data availability statement

The authors confirm that the data supporting the findings of this study are available within the article and its supplementary materials.

Disclosure statement

No potential conflict of interest was reported by the author(s).

Funding

This work was supported by the National Center for Research and Development TECHMATSTRATEG-III/0027/2019-00 grant and by the Research University Excellence Initiative at Adam Mickiewicz University by the grants: 121/08/POB2/0013, 030/07/POB2/0002, 100/19/POB2/0001, 037/02/POB2/0004.

References

[1] Jones JC, Burks R, Owens BD, et al. Incidence and risk factors associated with meniscal injuries Among active-duty US military service members. J Athl Train. 2012;47:67–73. doi:10.4085/1062-6050-47.1.67

[2] Nielsen AB, Yde J. Epidemiology of acute knee injuries: a prospective hospital investigation. The Jpurnal of Trauma. 1991;31; doi:10.1097/00005373-199112000-00014

[3] Thein R, Hershkovich O, Gordon B, et al. The prevalence of cruciate ligament and meniscus knee injury in young adults and associations with gender, body mass index, and height a large cross-sectional study. J Knee Surg. 2017;30:565–570. doi:10.1055/s-0036-1593620

[4] Mitchell J, Graham W, Best TM, et al. Epidemiology of meniscal injuries in US high school athletes between 2007 and 2013. Knee Surg Sports Traumatol Arthrosc. 2016;24:715–722. doi:10.1007/s00167-015-3814-2

[5] Logerstedt DS, Scalzitti DA, Bennell KL, et al. Knee pain and mobility impairments: meniscal and articular cartilage lesions revision 2018. J Orthop Sports Phys Ther. 2018;48:A1–A50. doi:10.2519/jospt.2018.0301

[6] Doral MN, Bilge O, Huri G, et al. Modern treatment of meniscal tears. EFORT Open Rev. 2018;3:260–268. doi:10.1302/2058-5241.3.170067

[7] Semba JA, Mieloch AA, Rybka JD. Introduction to the state-of-the-art 3D bioprinting methods, design, and applications in orthopedics. Bioprinting. 2020;18:e00070, doi:10.1016/j.bprint.2019.e00070

[8] Ng WL, Chua CK, Shen YF. Print Me An organ! Why We Are Not there Yet. Prog Polym Sci. 2019;97:101145, doi:10.1016/j.progpolymsci.2019.101145

[9] Cui X, Li J, Hartanto Y, et al. Advances in extrusion 3D bioprinting: a focus on multicomponent hydrogel-based bioinks. Adv Healthc Mater. 2020;9:1901648, doi:10.1002/adhm.201901648

[10] Ozbolat IT, Hospodiuk M. Current advances and future perspectives in extrusion-based bioprinting. Biomater. 2016;76:321–343. doi:10.1016/j.biomaterials.2015.10.076

[11] Ng WL, Yeong WY, Naing MW. Polyvinylpyrrolidone-Based Bio-Ink improves cell viability and homogeneity during drop-On-demand printing. Materials (Basel). 2017;10; doi:10.3390/ma10020190

[12] Bartolo P, Malshe A, Ferraris E, et al. 3D bioprinting: materials, processes, and applications. CIRP Ann. 2022;71:577–597. doi:10.1016/j.cirp.2022.06.001

[13] Li W, Mille LS, Robledo JA, et al. Recent advances in formulating and processing biomaterial inks for Vat polymerization-based 3D printing. Adv Healthc Mater. 2020;9:2000156, doi:10.1002/adhm.202000156

[14] Park SH, Jung CS, Min BH. Advances in three-dimensional bioprinting for hard tissue engineering. Tissue Eng Regen Med. 2016;13:622–635. doi:10.1007/s13770-016-0145-4

[15] Bandyopadhyay A, Ghibhela B, Mandal BB. Current advances in engineering meniscal tissues: insights into 3D printing, injectable hydrogels and physical stimulation based strategies. Biofabrication. 2024; doi:10.1088/1758-5090/ad22f0

[16] Elomaa L, Almalla A, Keshi E, et al. Rise of tissue- and species-specific 3D bioprinting based on decellularized extracellular matrix-derived bioinks and bioresins. Biomater Biosyst. 2023;12:100084, doi:10.1016/j.bbiosy.2023.100084

[17] Yi S, Ding F, Gong L, et al. Extracellular matrix scaffolds for tissue engineering and regenerative medicine. Curr Stem Cell Res Ther. 2017;12:233–246. doi:10.2174/1574888X11666160905092513

[18] Kusindarta DL, Wihadmadyatami H. The Role of Extracellular Matrix in Tissue Regeneration. In: Hussein Abdel hay El-Sayed Kaoud, editor. *Tissue Regeneration*. London: InTech; 2018. doi:10.5772/intechopen.75728

[19] Kim JW, Nam SA, Yi J, et al. Kidney Decellularized Extracellular Matrix Enhanced the Vascularization and Maturation of Human Kidney Organoids. Adv Sci. 2022;9:2103526, doi:10.1002/advs.202103526

[20] Ahn J, Sen T, Lee D, et al. Uterus-derived decellularized extracellular matrix-mediated endometrial regeneration and fertility enhancement. Adv Funct Mater. 2023;33:2214291, doi:10.1002/adfm.202214291

[21] Saldin LT, Cramer MC, Velankar SS, et al. Extracellular matrix hydrogels from decellularized tissues: structure and function. Acta Biomater. 2017;49:1–15. doi:10.1016/j.actbio.2016.11.068

[22] Meng X, Zhou Z, Chen X, et al. A sturgeon cartilage extracellular matrix-derived bioactive bioink for tissue engineering applications. Int J Bioprint. 2023;9:768, doi:10.18063/ijb.768

[23] Chakraborty J, Roy S, Ghosh S. Regulation of decellularized matrix mediated immune response. Biomater Sci. 2020;8:1194–1215. doi:10.1039/C9BM01780A

[24] Roosens A, Somers P, De Somer F, et al. Impact of detergent-based decellularization methods on porcine tissues for heart valve engineering. Ann Biomed Eng. 2016;44:2827–2839. doi:10.1007/s10439-016-1555-0

[25] Chen T-A, Sharma D, Jia W, et al. Detergent-Based decellularization for anisotropic cardiac-specific extracellular matrix scaffold generation. Biomimetics. 2023;8; doi:10.3390/biomimetics8070551

[26] White LJ, Taylor AJ, Faulk DM, et al. The impact of detergents on the tissue decellularization process: a ToF-SIMS study. Acta Biomater. 2017;50:207–219. doi:10.1016/j.actbio.2016.12.033

[27] Fernández-Pérez J, Ahearne M. The impact of decellularization methods on extracellular matrix derived hydrogels. Sci Rep. 2019;9:14933, doi:10.1038/s41598-019-49575-2

[28] Keane TJ, Swinehart IT, Badylak SF. Methods of tissue decellularization used for preparation of biologic scaffolds and in vivo relevance. Methods. 2015;84:25–34. doi:10.1016/j.ymeth.2015.03.005

[29] Mendibil U, Ruiz-Hernandez R, Retegi-Carrion S, et al. Tissue-Specific decellularization methods: rationale and strategies to achieve regenerative compounds. Int J Mol Sci. 2020;21; doi:10.3390/ijms21155447

[30] McHugh MA, Krukonis VJ. 9 - Polymers and monomers processing, in: M.A. McHugh, V.J.B.T.-S.F.E. (Second E. Krukonis (Eds.), Butterworth-Heinemann, Boston, 1994: pp. 189–292. doi:10.1016/B978-0-08-051817-6.50012-6.

[31] Davies OR, Lewis AL, Whitaker MJ, et al. Applications of supercritical CO2 in the fabrication of polymer systems for drug delivery and tissue engineering. Adv Drug Deliv Rev. 2008;60:373–387. doi:10.1016/j.addr.2006.12.001

[32] de Wit RJJ, van Dis DJ, Bertrand ME, et al. Scaffold-based tissue engineering: supercritical carbon dioxide as an alternative method for decellularization and sterilization of dense materials. Acta Biomater. 2023;155:323–332. doi:10.1016/j.actbio.2022.11.028
[33] Veryasova NN, Lazhko AE, Isaev DE, et al. Supercritical carbon dioxide-A powerful tool for green biomaterial chemistry. Russ J Phys Chem B. 2019;13:1079–1087. doi:10.1134/S1990793119070236
[34] Guler S, Aslan B, Hosseinian P, et al. Supercritical carbon dioxide-assisted decellularization of aorta and cornea. Tissue Eng Part C Methods. 2017;23:540–547. doi:10.1089/ten.tec.2017.0090
[35] Duarte MM, Silva IV, Eisenhut AR, et al. Contributions of supercritical fluid technology for advancing decellularization and postprocessing of viable biological materials. Mater Horiz. 2022;9:864–891. doi:10.1039/D1MH01720A
[36] Seo Y, Jung Y, Kim SH. Decellularized heart ECM hydrogel using supercritical carbon dioxide for improved angiogenesis. Acta Biomater. 2018;67:270–281. doi:10.1016/j.actbio.2017.11.046
[37] Duval K, Grover H, Han LH, et al. Modeling physiological events in 2D vs. 3D cell culture. Physiology. 2017;32:266–277. doi:10.1152/physiol.00036.2016
[38] Baker BM, Chen CS. Deconstructing the third dimension – how 3D culture microenvironments alter cellular cues. J Cell Sci. 2012;125:3015–3024. doi:10.1242/jcs.079509
[39] Cissell DD, Link JM, Hu JC, et al. A modified hydroxyproline assay based on hydrochloric acid in ehrlich's solution accurately measures tissue collagen content. Tissue Eng Part C Methods. 2017;23:243–250. doi:10.1089/ten.tec.2017.0018
[40] Semba JA, Mieloch AA, Tomaszewska E, et al. Formulation and evaluation of a bioink composed of alginate, gelatin, and nanocellulose for meniscal tissue engineering. Int J Bioprint. 2022;9:621, doi:10.18063/ijb.v9i1.621
[41] Teixeira AM, Martins P. Mechanical characterisation of an organic phantom candidate for breast tissue. J Biomater Appl. 2020;34:1163–1170. doi:10.1177/0885328219895738
[42] Crapo PM, Gilbert TW, Badylak SF. An overview of tissue and whole organ decellularization processes. Biomaterials. 2011;32:3233–3243. doi:10.1016/j.biomaterials.2011.01.057
[43] Reilly GC, Engler AJ. Intrinsic extracellular matrix properties regulate stem cell differentiation. J Biomech. 2010;43:55–62. doi:10.1016/j.jbiomech.2009.09.009
[44] Gattazzo F, Urciuolo A, Bonaldo P. Extracellular matrix: a dynamic microenvironment for stem cell niche. Biochim Biophys Acta Gen Subj. 2014;1840:2506–2519. doi:10.1016/j.bbagen.2014.01.010
[45] Cesarz Z, Tamama K. Spheroid Culture of Mesenchymal Stem Cells. Stem Cells Int. 2016;2016; doi:10.1155/2016/9176357
[46] Chae S, Lee SS, Choi YJ, et al. 3D cell-printing of biocompatible and functional meniscus constructs using meniscus-derived bioink. Biomaterials. 2021;267:120466, doi:10.1016/j.biomaterials.2020.120466
[47] Antons J, Marascio MGM, Nohava J, et al. Zone-dependent mechanical properties of human articular cartilage obtained by indentation measurements. J Mater Sci Mater Med. 2018;29; doi:10.1007/s10856-018-6066-0
[48] Bąkowski P, Mieloch AA, Porzucek F, et al. Meniscus repair via collagen matrix wrapping and bone marrow injection: clinical and biomolecular study. Int Orthop. 2023;47:2409–2417. doi:10.1007/s00264-023-05711-2
[49] Le LTT, Pham CN, Trinh X-T, et al. Supercritical carbon dioxide decellularization of porcine nerve matrix for regenerative medicine. Tissue Eng Part A. 2024; doi:10.1089/ten.TEA.2023.0228
[50] Reis DP, Domingues B, Fidalgo C, et al. Bioinks enriched with ECM components obtained by supercritical extraction. Biomolecules. 2022;12:394, doi:10.3390/biom12030394
[51] Sevastianov VI, Nemets E, Lazhko A, et al. Application of supercritical fluids for complete decellularization of porcine cartilage. J Phys Conf Ser. 2019;1347; doi:10.1088/1742-6596/1347/1/012081
[52] Mori L, Libero GD. Presentation of lipid antigens to T cells. Immunol Lett. 2008;117:1–8. doi:10.1016/j.imlet.2007.11.027
[53] Win TS, Crisler WJ, Dyring-Andersen B, et al. Immunoregulatory and lipid presentation pathways are upregulated in human face transplant rejection. J Clin Invest. 2021;131, doi:10.1172/JCI135166
[54] Piontek T, Ciemniewska-Gorzela K, Naczk J, et al. Complex meniscus tears treated with collagen matrix wrapping and bone marrow blood injection. Cartilage. 2016;7:123–139. doi:10.1177/1947603515608988
[55] Ciemniewska-Gorzela K, Bąkowski P, Naczk J, et al. Complex meniscus tears treated with collagen matrix wrapping and bone marrow blood injection: clinical effectiveness and survivorship after a minimum of 5 years' follow-Up. Cartilage. 2021;13:228S–238S. doi:10.1177/1947603520924762
[56] Ritchie RDR, Salmon SL, Hiles MC, et al. Lack of immunogenicity of xenogeneic DNA from porcine biomaterials. Surg Open Sci. 2022;10:83–90. doi:10.1016/j.sopen.2022.07.005
[57] Jian Z, Zhuang T, Qinyu T, et al. 3D bioprinting of a biomimetic meniscal scaffold for application in tissue engineering. Bioact Mater. 2021;6:1711–1726. doi:10.1016/j.bioactmat.2020.11.027
[58] Romanazzo S, Vedicherla S, Moran C, et al. Meniscus ECM-functionalised hydrogels containing infrapatellar fat pad-derived stem cells for bioprinting of regionally defined meniscal tissue. J Tissue Eng Regen Med. 2018;12:e1826–e1835. doi:10.1002/term.2602
[59] Mieloch AA, Semba JA, Rybka JD. CNT-Type dependent cellular adhesion on 3D-printed nanocomposite for tissue engineering. Int J Bioprint. 2024;8:548–79. doi:10.18063/ijb.v8i2.548